J Mater Sci (2011) 46:1289–1294
DOI 10.1007/s10853-010-4913-6

The improvement of the amorphous environment of the germanate–tellurate glasses in the presence of the gadolinium ions

S. Rada · R. Chelcea · M. Culea · E. Culea

Received: 13 April 2010 / Accepted: 9 September 2010 / Published online: 24 September 2010

Abstract Glasses in the system $x\mathrm{Gd_2O_3}\cdot(100-x)[\mathrm{TeO_2}\cdot\mathrm{GeO_2}]$ with $0 \leq x \leq 50$ mol% have been prepared from melt quenching method. In this paper, we investigated changes of the coordination numbers of germanium, tellurium, and gadolinium ions by investigations of FTIR, EPR, and UV–VIS spectroscopy. By analyzing the structural changes resulted from the IR spectra we found that the bending modes of [GeO_4] structural units and the deformed modes of the Te–O–Te linkages produce intercalation of the [GdO_n] entities in the germanate–tellurate chain network and densification of the glasses by increasing the number of [GeO_6] structural units. EPR spectra of the studied samples reveal that the gadolinium ions play a role of network former. The UV–VIS spectra show broad UV absorption bands located in the 250–350 nm region. Their intensity increase with the increasing of Gd_2O_3 content showing that these stronger transitions can be due to the presence of the O=Ge bonds (n–π* excitations) of [GeO_5] structural units. The [GeO_5] structural units are more stable thermodynamically than their analogues and the [GeO_6] structural units produce the improvement of the amorphous character of these glasses.

Introduction

Germanate glasses doped with rare earth ions were investigated extensively in the past because their physicochemical, optical, and spectroscopic properties are advantageous for optoelectronic applications [1–4].

Tellurium oxide is a heavy metal oxide, and when it is introduced in the glass matrix, it may influence the physical properties as refractive index, thermal expansion coefficient, chemical resistance, infrared transmittance of the glasses and further makes the glasses suitable for use as devices for communication and advanced computer applications. When doped with a different kind of rare earth ions, these glasses find wide use in high power laser technology, sensor, optical switching, and amplifiers for fiber communications [5–7].

It is expected that the introduction of rare-earth oxide component into the binary germanate–tellurate glasses may affect the structural features of the host matrix. Thus, it can be thought that the behavior of the properties of binary germanate glasses at increasing the second component content would depend on how that component influences the glass polymerization pattern.

The purpose of this paper is to understand the amorphous environment of the gadolinium–germanate–tellurate glasses using the FTIR, EPR, and UV–VIS spectroscopy investigations.

Experimental

Gadolinium–germanate–tellurate glasses were prepared by mixing and melting of the appropriate amounts of tellurium dioxide, germanium dioxide, and gadolinium (III) oxide of

S. Rada (✉) · R. Chelcea · E. Culea
Department of Physics, Technical University of Cluj-Napoca,
400641 Cluj-Napoca, Romania
e-mail: Simona.Rada@phys.utcluj.ro; radasimona@yahoo.com

M. Culea
Faculty of Physics, Babes-Bolyai University,
400084 Cluj-Napoca, Romania

high purity. Reagents were melted at 1000 °C for 15 min and quenched.

The samples were analyzed by means of X-ray diffraction using a XRD-6000 Shimadzu Diffractometer, with a monochromator of graphite for Cu Kα radiation ($\lambda = 1.54$ Å) at room temperature. The X-ray diffraction patterns did not reveal the crystalline phase in the sample with $x \leq 50$ mol% Gd_2O_3.

The structure of the glasses was investigated by infrared transmission spectra in KBr matrices were recorded in the range 400–1200 cm^{-1} using a JASCO FTIR 6200 spectrometer.

UV–Visible absorption spectra of the powdered glass samples were recorded at room temperature in the range 250–400 nm using a Perkin-Elmer Lambda 45 UV/VIS spectrometer. These measurements were made on glass powder dispersed in KBr pellets.

EPR measurements were performed at room temperature using ADANI Portable EPR PS 8400-type spectrometer, in X frequency band (9.1 GHz) and a field modulation of 100 kHz. The microwave power used was 5 mW.

Results and discussion

FTIR spectroscopy

A simple inspection of the IR spectra presented in Fig. 1 shows that the structural properties are the result of changes in the short-range order of the gadolinium–germanate–tellurate glasses. These modifications can be summarized as follows:

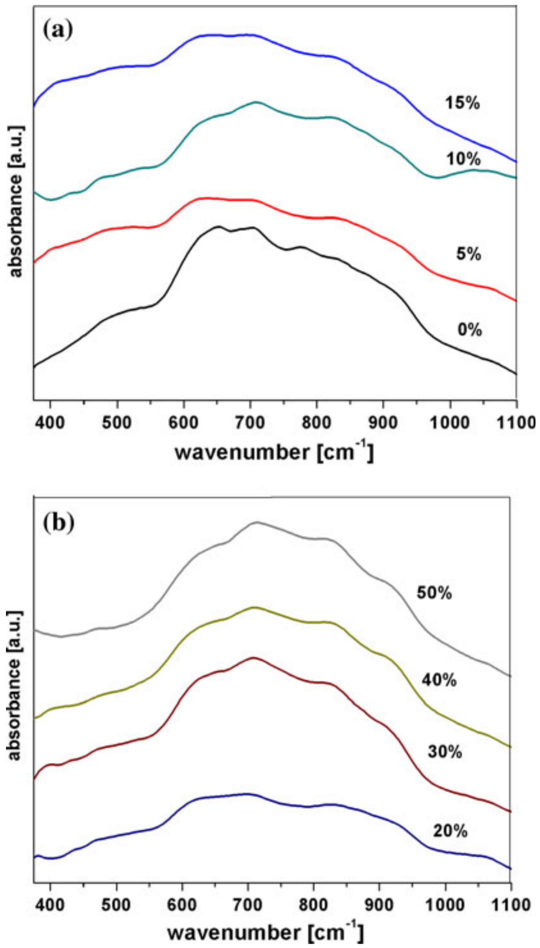

Fig. 1 FTIR spectra of the $x Gd_2O_3 \cdot (100 - x)[TeO_2 \cdot GeO_2]$ glasses (with $x = 0$–50 mol%)

(i) The bands in the 400–500 cm^{-1} region consists of various bands due to stretching and bending modes of the [GeO_4] structural units and the vibrations of Te–O–Te bridging bonds [8–16]. For sample with $x \geq 15$ mol% Gd_2O_3, these bands attain their maximum values. This shows that the bending modes of [GeO_4] structural units and the deformed modes of the Te–O–Te linkages produce intercalations of the [GdO_n] entities in the germanate–tellurate chain network.

(ii) The band located at about 780 cm^{-1} shows the presence of [TeO_3] structural units [8–10]. The intensity of this band attains maximum value for host matrix network. This shows that the gadolinium ions are firstly inserted in the trivalent state and they can be considered as modifiers because they have a strong affinity toward these groups containing non-bridging oxygens, with negative electric charges. Presence of multiple cations, germanium, and tellurium in the glasses to attract oxygen ions produce a competition between these cations. The disappearance of this band relates that gadolinium ions have an affinity pronounced toward [TeO_3] structural units yielding deformation of the Te–O–Te linkages and the intercalation of the [GdO_n] entities in the [TeO_4] chain network.

(iii) The feature of the band located at about ~700 cm^{-1} is attributed to the vibrations of the Ge–O bonds from the [GeO_6] structural units. For samples with $x = 10$, 30 and 50 mol% Gd_2O_3 increases the intensity of this band.

(iv) The characteristic feature located at about ~820 cm^{-1} can be due to the Ge–O stretching vibrations of the [GeO_4] tetrahedral structural units involving non-bridging oxygen [10, 11].

(v) The IR absorption bands in the 700–970 cm^{-1} region were found to be sensitive for the different germanate units in the form of [GeO_4], [GeO_6] structural units and interconnected through Ge–O–Ge bridges in [GeO_4] structural units [14]. The bands located in the 930 and 1020 cm^{-1} range were assigned to the Ge–O and Ge–O–Ge stretching vibrations from $[GeO_4]$ structural units [15–19].

(vi) The band centered at $\sim$650 cm^{-1} is assigned to the stretching mode of $[TeO_4]$ trigonal bipyramidal units with the bridging oxygen [8–10]. When a small Gd_2O_3 content (5 mol%) is introduced in host network, the characteristic features of these specific units of tellurium atoms are affected and the band shifts to the lower wavenumbers. The effect suggests that doping with gadolinium ions deforms the Te–O–Te linkages and some $[TeO_3]$ structural units are converted to $[TeO_4]$ structural units while the number of the $[GeO_6]$ structural units decreases (the band located at about 700 cm^{-1}).

By increasing the Gd_2O_3 content up to 10 mol%, the evolution of the structure can be explained considering the accommodation of the network with excess of oxygen by the formation of $[GeO_6]$ structural units.

Then by the increasing of Gd_2O_3 content up to 20 mol% a sharp of decreasing trend was observed in intensity of the band situated in the 700 cm^{-1} region and new increasing trends towards larger wavenumber were exposed on the bands centered in the 800–950 cm^{-1} region. Structural changes, as recognized by analyzing band shapes of FTIR spectra, revealed that Gd_2O_3 causes a change from the continuous germanium–tellurate network to the continuous germanate–tellurate network with interconnected through Ge–O–Ge, Te–O–Te, and Ge–O–Te bridges.

The currently accepted model for this mechanism is a change of germanium from four-coordinated to higher coordinated species ($x \leq 10$ mol%) after that the number of $[GeO_6]$ structural units decreases ($10 < x \leq 20$ mol%). This structural mechanism is responsible for the germanate anomaly with remains area of interest to the glass science [12, 13].

The germanate anomaly consists in a growth followed by a decline of the number of $[GeO_6]$ octahedral structural units in the glass network [10–14]. While the formation of the higher coordinated species clearly plays a role in the anomalous behavior it does not correlate with the anomaly maximum. Some authors consider that germanate anomaly can be correlated with the existence of five-coordinated germanium atoms $[O_4Ge{=}O]$ or a mixture of five and six-coordinated.

An important question to be considered is if the diffraction experiments reveal the presence of $[GeO_5]$ polyhedrons. With a few exceptions [17, 20], only $[GeO_6]$ and $[GeO_4]$ structural units were found in the related crystalline structures. The simple models for the increased coordination number of the germanium–oxygen bonds are based on these two structural units. Distorted $[GeO_5]$ trigonal bipyramids with one longer Ge–O bond exist in the $K_2Ge_8O_{17}$ crystal [17], but the pyramidal apices are connected with special four-coordinated oxygen, an unlikely site in a glass structure, and so these crystalline parameters were not used in the structural comparisons.

Further, by increasing of gadolinium oxide content up to 50 mol%, the intensity of the band centered at about 700 cm^{-1} increases. These mechanisms relate that when a high content of Gd_2O_3 ($\geq$30 mol%) is introduced, the Te–O–Te linkages are deformed yielding intercalation of $[GdO_n]$ entities. The bending mode of the $[GeO_4]$ structural units permits the accommodation of the network with excess of oxygens ions by the formation of $[GeO_6]$ structural units. These data will be used in the present research to understand the FTIR data concerning the local environment of the gadolinium ions using EPR spectroscopy.

EPR spectroscopy

Figure 2 shows the EPR spectra of $xGd_2O_3{\cdot}(100-x)[TeO_2{\cdot}GeO_2]$ glasses sample as function of gadolinium

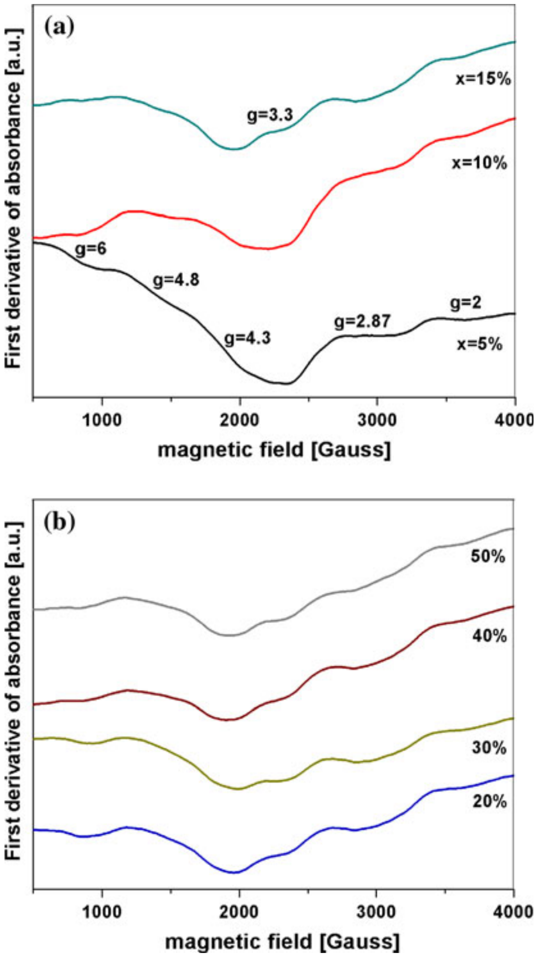

Fig. 2 EPR spectra of the $xGd_2O_3{\cdot}(100-x)[TeO_2{\cdot}GeO_2]$ glasses

ions concentration. The Gd^{+3} ions doped germanate–tellurate glasses exhibit six resonance signals at $g \approx 2.0$, 2.8, 3.3, 4.3, 4.8, and 6.

Most of the authors [20–25] consider that when the gadolinium ions present in low concentrations in host glasses, usually exhibit three prominent signals with effective g-values of $g \approx 6$, 2.8, and 2.0 superimposed on a broad resonance line shape that encompasses the prominent $g \approx 2.0$ resonance signals. The mentioned absorption features are generated by Gd^{+3} ions disposed in cubic, octahedral, or tetrahedral sites with moderate distortions. In these sites the gadolinium ions experience a relatively weak crystalline field and they are characterized by a coordination number higher than six [23–25].

The asymmetric absorption line with $g \approx 4.8$ indicates a relatively strong crystal field with an orthorhombic symmetry and is associated with gadolinium ions with a coordination number lower than six [22].

In addition to the signals at $g \approx 3.3$ and 4.3 are also observed [20]. This type of spectrum has been aptly labeled as the U-spectrum [23] in view of its omnipresence in vitreous materials [20–28] as well as in disordered polycrystalline materials.

In the present work, the increase of Gd_2O_3 content does modify the characteristic bands of the EPR spectra and can be characterized as follows:

(i) The intensity of the EPR signal located at $g \approx 3.3$ is weak. For sample with $x \geq 15$ mol%, the EPR spectra show all absorption features of the U-spectrum. This explains that the amorphous character of the glasses increase by increasing of the gadolinium ions.

(ii) The resonance line located at about $g \approx 4.8$ increases by increasing of Gd_2O_3 content. This shows that the type of the Gd^{+3} ions can be presented as network former in the host matrix.

(iii) Moreover, we observed a weak resonance line attributed the $g \approx 2$ due to formation of Gd^{+3} clusters for all glasses. The weak resonance line $g \approx 6$ was considered to be a characteristic feature of intermediate crystal field sites of axial symmetry and have attributed the broadened general appearance of the U-spectrum to isolated rare earth ions in wide varieties of sites. The Gd^{+3} ions in these glasses can be considered as isolated in the sense of the absence of clustering. The weakening intensity of the clusters EPR line could be due to the Gd^{+3} migrations inside the glass network. It should lead to the appearance of more Gd^{+3} content in network former positions. It can be pointed that the Gd^{+3} ions are generally suspected to improve their environment.

In brief, with the addition of Gd_2O_3 in the host matrix which tend to coordinate with Gd^{+3}, will contribute to coordinate with glass former cation ions. According to the electronegativity theory, the covalency of the bond will become stronger with the decrease of the difference of electronegativity between cation and anion ions. Since the values of electronegativity, for Te, Ge, Gd, and O elements are 2.1, 1.8, 1.3, and 3.5, respectively, the covalency of Te–O are stronger than Ge–O and Gd–O, respectively. As a result, the covalency of Te–O and Ge–O bonds is stronger than that of the Gd–O bond.

Accordingly, the excess of non-bridging oxygen ions will coordinate with gadolinium ions only after what the tellurium and germanium cations attain maximum number of coordination (tellurium atoms—4 and germanium atoms—6), in agreement with our FTIR data. In accordance to the EPR data, the Gd^{+3} ions in these glasses can be considered as isolated in the sense of the absence of clustering.

UV–VIS spectroscopy

Incorporation of germanium ions in the glass was allowed photosensitivity effects with applications in the telecommunications, lasers, and sensors. Photosensitivity has been explained by two mechanisms [29]: (i) the formation of new paramagnetic defects after UV laser irradiation, depending on glass composition; (ii) the densification of the glasses which can be correlated by the increase of refractive index.

The term of densification of the glass implies a change in coordination of Ge^{+4} ions from four- to sixfold which will lead to glass compaction and then to refractive index increase. Accordingly, our gadolinium–germanate–tellurate glasses can present the optical properties.

The UV–VIS absorption spectra of $x Gd_2O_3 \cdot (100 - x)[TeO_2 \cdot GeO_2]$ glasses are shown in Fig. 3. The energy of

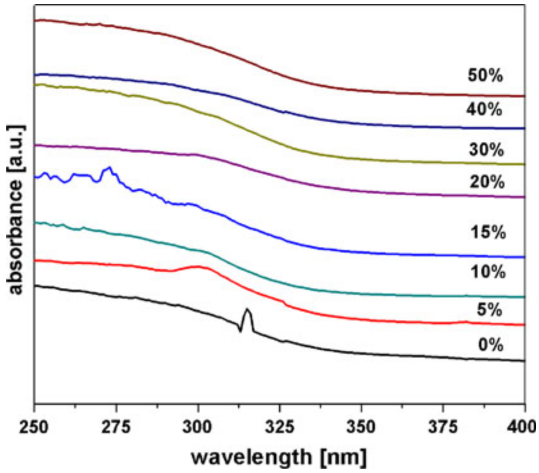

Fig. 3 UV–VIS absorption spectra of samples in function of gadolinium oxide content

ultraviolet (>250 nm) and visible radiation is sufficiently to promote the bonding π orbital—antibonding π^* orbital and non-bonding orbital (oxygen ions)—antibonding π^* orbital excitations. The examinations of these spectra show that the characteristic UV–VIS bands are modified namely:

(i) It follows from the spectrum that all glasses show the beginning absorption at about 250 nm. This band can be due to the presence of Ge–Ge wrong bonds [30].

(ii) For sample with $x = 5$ mol%, a new band located at about 285 nm appears in the UV–VIS spectrum. This band could be related to the presence of gadolinium ions in the glass, which could contribute to form gadolinium germanate-like structure [29].

(iii) For sample with $x = 15$ mol% Gd_2O_3, stronger electronic transitions can be observed in the 200–300 nm region. The intensity of the UV–VIS signal increases with the increasing of the Gd_2O_3 content up to 50 mol% in the host matrix. By comparing with FTIR data, for sample with $x = 15$ mol% can be observed that the number of six-coordinated atoms decrease. This shows the existence of the germanate anomaly. Then, by increasing of Gd_2O_3 content up to 50 mol% the number of $[GeO_6]$ structural units increase again. Accordingly, these stronger transitions in the UV–VIS spectrum can be due to the presence of the $[O_4Ge{=}O]$ structural units. The O=Ge bond of $[GeO_5]$ structural units show strong absorption in the ultraviolet due to allowed n–π^* transition. The $[GeO_5]$ structural units are more stable thermodynamically than their analogues [31, 32] and the $[GeO_6]$ structural units produce the improvement of the amorphous character of these glasses.

We assume that $[GeO_5]$ and/or $[GeO_6]$ structural units also do not accommodate with the non-bridging oxygens, and that the $[GdO_n]$ polyhedrons are suitable neighbors for the germanate structural units, in agreement with the UV–VIS data.

Conclusions

Homogeneous glasses of $x\mathrm{Gd_2O_3}\cdot(100 - x)[\mathrm{TeO_2}\cdot\mathrm{GeO_2}]$ system were obtained within $0 \leq x \leq 50$ mol%. In this paper, we investigated changes in structural properties of the gadolinium–germanate–tellurate glasses through investigations of FTIR, EPR, and UV–VIS spectroscopy.

Our results show that the formation of $[GeO_6]$ structural units attains maximum value at 10 mol% Gd_2O_3, after that decreases (for sample with $x = 15$–20 mol%) and then, increases again. Accordingly, the excess of non-bridging oxygen ions will coordinate with gadolinium ions only after what the tellurium and germanium cations attain maximum number of coordination.

EPR data show that the Gd^{+3} ions in these glasses can be considered as isolated in the sense of the absence of clustering. The broader UV absorption bands located in the 250–350 nm region corresponds to the formation of gadolinium germanate-like structure.

Acknowledgements The financial support of the Ministry of Education and Research of Romania-National University Research Council (CNMP, Parteneriate, contract number 71099/2007) is gratefully acknowledged by the authors.

References

1. Mendez-Ramos J, Lavin V, Martin IR, Rodriguez-Mendoza UR, Gonzales-Almeida JA, Rodríguez VD, Lozano-Gorrin AD, Nunez P (2001) J Alloys Compd 323&324:753
2. Bueno LA, Melnikov P, Messadeg Y, Ribeiro SJL (1999) J Non-Cryst Solids 247:87
3. Guinhos FC, Nobrega PC, Santa-Cruz PA (2001) J Alloys Comp 323&324:358
4. Wachtler M, Spegini A, Gatterer K, Fritzer HP, Ajo D, Bettinelli M (1998) J Am Ceram Soc 81:2045
5. Weber MJ (1990) J Non-Cryst Solids 123:208
6. Jiang S, Myers M, Peyghambarian N (2000) J Non-Cryst Solids 263:3
7. Ajithkumar G, Gupta PK, Jose G, Unnikrishnan NV (2000) J Non-Cryst Solids 275:93
8. Rada S, Culea M, Culea E (2008) J Phys Chem A 112(44):11251
9. Rada S, Rada M, Culea E (2010) Spectrochim Acta A 75:846
10. Rada S, Culea M, Rada M, Culea E (2010) J Alloys Compd 490:270
11. Rada S, Culea M, Culea E (2008) J Non-Cryst Solids 354(52–54):5491
12. Rada S, Culea E, Rada M, Pascuta P, Maties V (2009) J Mater Sci 44:3235. doi:10.1007/s10853-009-3433-8
13. Rada S, Culea M, Rada M, Culea E (2008) J Mater Sci 43(18):6122. doi:10.1007/s10853-008-2939-9
14. Rada M, Culea E, Rada S, Maties V, Pascuta P (2010) J Mater Sci 45:1487. doi:10.1007/s10853-009-4109-0
15. Henderson GS (2007) J Non-Cryst Solids 353:1695
16. Henderson GS, Fleet ME (1991) J Non-Cryst Solids 134:259
17. Dimitrov V, Dimitriev Y, Montenero A (1994) J Non-Cryst Solids 180:51
18. Pascuta P, Pop L, Rada S, Bosca M, Culea E (2008) Vibrat Spectrosc 48:281
19. Blaszczak K, Adamczyk A (2001) J Mol Struct 596:61
20. Durand A, Mentre O, Abraham F, Fukuda T, Eloudi B (2006) Solid State Sci 8:155
21. Iton IE, Brodbeck CM, Suib SL, Stucky GD (1983) J Chem Phys 79:1185
22. Legein C, Buzare JY, Silly G, Jacoboni C (1996) J Phys Condens Matter 8:4339
23. Ardelean I, Griguta L (2007) J Non-Cryst Solids 353:2363
24. Culea E, Milea I (1995) J Non-Cryst Solids 189:246
25. Brodbeck CM, Iton IE (1985) J Chem Phys 83:4285
26. Kliava J, Edelman I, Potseluyko A, Petrakovskaja E, Berger R, Bruckental I, Yeshurun Y, Malakhovskii A, Zarubina T (2004) J Magn Magn Mater 272–276:E1647
27. koopmans HJA, Perie MM, Niuzenhuijse B, Gallings PJ (1993) Phys Status Solidi B 120:745

28. Furniss D, Harris EA, Hollis DB (1987) J Phys C: Solid State Phys 20:L147
29. Ferraris M, Milanese D, Contardi C, Chen Q, Menke Y (2004) J Non-Cryst Solids 347:246
30. Atkins RM, Mizrahi V (1992) Electron Lett 28:1742
31. Rada S, Culea E (2010) Mol Phys 108(14):1877
32. Rada S, Chelcea R, Culea M, Dehelean A, Culea E (2010) J Mol Struct 977:170